

CONTROL LAW OPTIMIZATION OF A RIGID-FLEXIBLE SATELLITE WITH A REACTION WHEEL USING THE MULTI-OBJECTIVE GENERALIZED EXTREMAL OPTIMIZATION WITH REAL CODIFICATION

Igor Mainenti Leal Lopes
rogimainenti@gmail.com
Luiz Carlos Gadelha de Souza
gadelha@dem.inpe.br
Fabiano Luis de Sousa
fabiano@dem.inpe.br

National Institute for Space Research – INPE
Av.dos Astronautas, 1758 – 12201-970 São José dos Campos – SP - Brazil

Abstract: *In this work, the efficiency of a multi-objective version of Generalized Extremal Optimization with real codification, called $M\text{-GEO}_{real}$, was tested by tackling an optimal attitude control problem of a rigid-flexible satellite. The satellite was controlled by a reaction wheel driven by a DC motor. $M\text{-GEO}_{real}$ was used to determine the gains of two control laws types (a proportional derivative (PD) and a non-linear control law) that minimize, simultaneously, the time and the energy to control the satellite. The performance of $M\text{-GEO}_{real}$ was compared to the Linear Quadratic Regulator (LQR) method. By that investigation one observes that $M\text{-GEO}_{real}$ is a very competitive approach to tackle this kind of problem, since it was able to obtain better solutions than LQR method.*

Keywords: *rigid-flexible satellite, non-linear control, evolutionary algorithm, multi-objective optimization.*

1 Introduction

Most of satellites need to be positioned with a certain attitude in order to fulfill their mission requirements (Hughes, 1986). Therefore, attitude control is one of most important system in the satellite. Nowadays, structures, like solar panels, need to be bigger to fulfill the energy requisites and the total mass of the satellite needs to be lower to reduce the satellite cost. These conditions make the space structures more complex, since it becomes more flexible. Such flexible structures increase the difficulty to the attitude control system performs its job. One of the problems tackle by the attitude control system of flexible structure is to make attitude maneuvers, keeping the level of pointing accuracy and the residual vibration after that operation (DeSouza, 2006). In this way, better methods capable to develop this system become necessary. In this context, it is interesting to test new algorithms capable to obtain optimized control laws.

A kind of optimization algorithms that has been widely used in engineering and scientific optimization problem is the evolutionary algorithms (Davis *et al.*, 1999; Ge and Chen, 2004). Evolutionary algorithms are stochastic methods of optimization that is based on nature process. This kind stochastic method employs a population of candidate solutions that is “evolved” during the search as better individuals (new solutions) are generated from previous ones in the sense that they are closer to the global minimum. The main advantage of the evolutionary algorithms is the capacity to avoid local optimal solutions, allowing searching for the global optimum. In fact,

evolutionary algorithms are very robust methods. They are capable to tackle problems with non-linearities in the objective functions. They can easily deal with constraints and their non-linearities, and also deal well with problems that have differently kinds of design variable.

Recently, a new EA, called M-GEO_{real}, capable to tackle multi-objective problems was proposed (Mainenti-Lopes *et al.* 2009). This algorithm is a multi-objective version of the Generalized Extremal Optimization (GEO) algorithm (De Sousa *et al.*, 2003; De Sousa *et al.* 2004). M-GEO_{real} was developed to obtain the Pareto Front maintaining the main characteristics of GEO algorithm and using a real codification, instead of binary codification. This algorithm does not use derivatives during the search; can be applied to unconstrained or constrained problems and non-convex or even disjoint design spaces, in the presence of any combination of continuous, discrete or integer design variables.

In this work, the Multi-objective Generalized Extremal Optimization with real codification (M-GEO_{real}) is tested in the optimal attitude control of rigid-flexible satellite. The satellite was modeled as a central rigid body with a flexible beam clamped on it. The satellite model was based on the work of Mainenti-Lopes *et al.* (2009). However, in the present work, a reaction wheel driven by a DC motor was included in the satellite model. The reaction wheel was used to control the satellite attitude. Two control laws were tested: a proportional derivative and; a non-linear control law. M-GEO_{real} was used to determine the control laws gains that minimize the time to control the satellite and the energy spent on it. As result, the M-GEO_{real} returned the Pareto Front for the two cases of control laws and its performance was compared to the Linear Quadratic Regulator (LQR).

The paper is divided in six sections. In section 2, the M-GEO_{real} algorithm is described. In section 3, the satellite mathematical model is presented. Following by the definition of the control laws in section 4 and the objective functions in section 5. In section 6, the results are presented. Finally, section 7 concludes this work.

2 Multi-objective Generalized Extremal Optimization with real codification

Multi-objective optimizations problems consist in optimize simultaneously two or more conflicting objectives. One cannot obtain one solution that optimizes all objectives if the objectives are conflicting. Therefore, one can obtain a set of solutions that, for each solution, it is impossible to optimize one objective without losing optimality in the others. This set of solution in the design space is called Pareto Set and in the objective space is called Pareto Front. The main goal of an algorithm capable to tackle multi-objective problems is to obtain the Pareto Set and the Pareto Front.

In order to tackle such kind of problem was develop an algorithm called M-GEO_{real} (Mainenti-Lopes *et al.* 2009). It was based on an algorithm presented by Mainenti-Lopes *et al.* (2008), called GEO_{real2}. The main difference between GEO_{real2} and M-GEO_{real} is how each one deals with the best solution. As a mono-objective algorithm, GEO_{real2} stores the best solution along the run and returns only one solution. While M-GEO_{real} stores the non-dominated solutions along the run and for each new solution a test is made to determine which solution will be kept and which will be discarded. The following steps describe this test that will be called Pareto Front Test in this work:

(i) test if the new solution is dominated by any solution in the stored Pareto Front. That is, if any solution in Pareto Front is at least equal in all objective functions except for one that is better than

the new solution. If the new solution is dominated, keep the Pareto Front and go to the step (iii). Otherwise, include the new solution and go to the next step;
(ii) determine all solutions that the new solution dominate and discard them from the Pareto Front;
(iii) finish the Pareto Front Test.

M-GEO_{real} was developed to recover the Pareto Front and the Pareto Set maintaining the main characteristic of GEO algorithm. The M-GEO_{real} can be described by the following steps:

(i) initialize randomly a string of N design variables, calculate the value of all functions $F_m(\mathbf{x})$ with this set of variables, where m is the number of objective functions. Store $F_m(\mathbf{x})$ in Pareto Front and \mathbf{x} in Pareto Set;
(ii) set the value of the index i to 1;
(iii) set the value of the index j to 1;
(iv) generate randomly m weight w_m between 0 and 1, each one associate to each objective function and calculate the adaptability of \mathbf{x} given by

$$A_j = \frac{\sum_{k=1}^m w_k F_k(\mathbf{x})}{\sum_{k=1}^m w_k}. \quad (1)$$

with $j = 0$. A_0 represents the probability to maintain the variable value unchanged. That is, $x'_{i0} = x_i$. Therefore, there is a chance to keep the variable value if it is a good value;

(v) Change the value of the variable x_i using an equation given by

$$x'_{ij} = x_i + N_j(0, \sigma_j)x_i \quad (2)$$

calculate $F_m(\mathbf{x})$ using the value of x'_{ij} instead of x_i and run the Pareto Front Test. Calculate the adaptability of x'_{ij} using the Eq. (1);

(vi) return the value x_i to the vector \mathbf{x} , increment the value of j , return to step (iv). Repeat this sequence until $j > P$;

(vii) assign a rank k_j to each x'_{ij} according to the A_j value with $j = 0, 1, \dots, P$, where $k_j = 1$ to the best value and $k_j = P + 1$ to the worst value;

(viii) chose with uniform probability one of x'_{ij} , accept this choice with probability equal to $k_j^{-\tau}$. If the choice was accepted store the chosen x'_{ij} , but do not change the value of x_i yet, and continue to next step. In the other wise, repeat this step;

(ix) increment the index i and go back to step (iii). Repeat this process until $i > N$.

(x) change each element x_i of the vector \mathbf{x} according to the value x'_{ij} chosen in step (vii). Calculate $F_m(\mathbf{x})$ using the new vector \mathbf{x} and run the Pareto Front Test. Test a stopping criterion. If it was accepted go to step (xii). Otherwise, test a population restart criterion. If it is accepted go to step (xi). Otherwise, go back to step (ii);

(xi) initialize randomly a string of N design variables, calculate all objective function value $F_m(\mathbf{x})$ with this set of variables and run the Pareto Front Test. Go back to step (ii);

(xii) return the Pareto Front and the Pareto Set.

The flowchart of M-GEO_{real} is presented in Fig. 1.

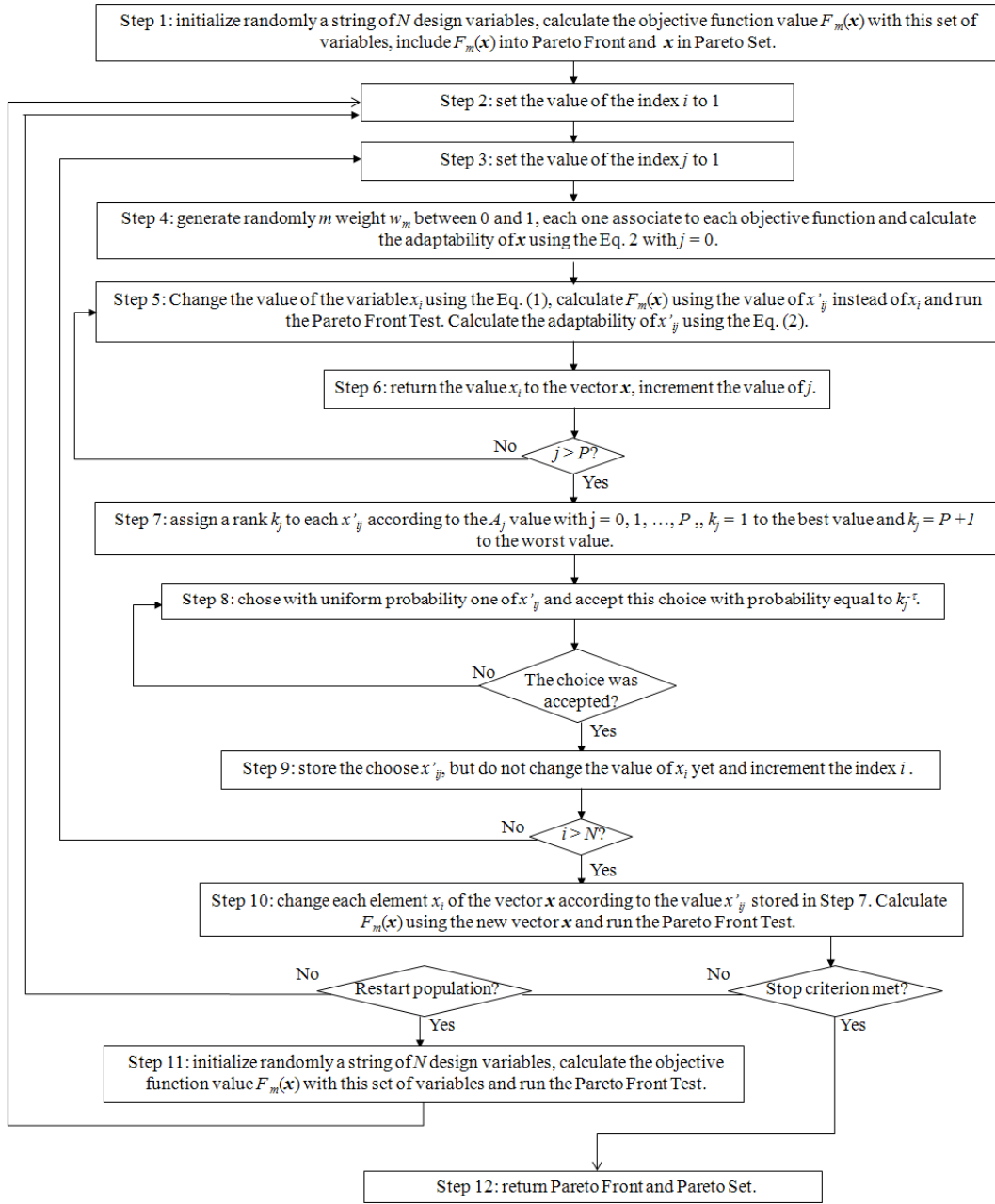


Figure 1. M-GEO_{real} flowchart.

The population restart test is made to increase the algorithm capacity to recover all Pareto Front. In this work, the criterion to restart the population was given by the free parameter rt that represents the number of restarts along the search.

Several values of standard deviation was used for the same variable to able the algorithm to search in a greater range of value in a single iteration. Therefore, it is interesting to select high and low values of σ_j . A feasible way to assure this and reduce the amount of free parameters is to adopt the following rule

$$\sigma_{i+1} = \frac{\sigma_i}{s.i} \quad (3)$$

where $i = 1, 2, \dots, P$ and s is a arbitrary number greater than one. In this work, the value of s was 2. In that way, one needs to define only σ_1 and all the other values of σ_j will be automatically defined. Therefore, there are as many high values as low values of σ . In this way, one needs to define four free parameters σ_1, P, τ and rt .

This algorithm will be used to tackle a satellite control optimization problem. In this problem, two objectives need to be optimized simultaneously: the time to control the satellite and the energy spent to do such job. The mathematical development of this satellite is presented in next section.

3 Mathematical model for a rigid-flexible satellite

The satellite was modeled as flexible beam clamped in a rigid body. The flexible beam represents a satellite flexible antenna or solar panel, while the rigid body represents the satellite central body. This system is controlled by a DC motor that drives a reaction wheel. The satellite model was based in a model used by Mainenti-Lopes *et al.* (2009) including a simple model of the DC motor. The satellite rigid body was modeled as a cube with edge equal to 1 m with a flexible beam of 1.2 m clamped in one of its edge. The satellite is free to rotate only in the XY plane. A graphic representation of the satellite model in XY plane is presented in Fig. 2.

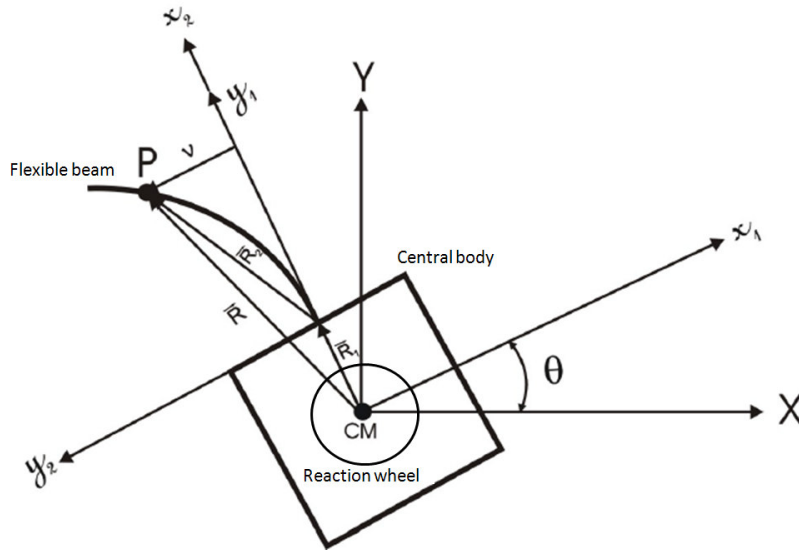


Figure 2. Graphic representation of the rigid-flexible satellite.

In order to model the flexible beam, it was used an Euler-Bernoulli formulation (Rezende *et al.*, 2004). Considering only the first vibration mode of the beam and using a lagrangian formulation, the system rigid body plus flexible beam can be described by the following equations

$$\begin{cases} 2C_3\ddot{\theta} + C_2\ddot{p} + 2C_1p^2\ddot{\theta} + 4C_1\dot{\theta}p\dot{p} = \xi \\ 2C_1\ddot{p} + C_2\ddot{\theta} - 2C_1\dot{\theta}^2p + 2C_1\omega^2p = 0 \end{cases} \quad (4)$$

where p is the modal state, θ is the rotation angle of the central body, ω is the beam first mode of vibration and C_1 , C_2 and C_3 are constants given by

$$C_1 = \frac{\rho A_h}{2} \quad (5)$$

$$C_2 = \rho A_h R_1 \lambda + \rho A_h \mu \quad (6)$$

$$C_3 = \frac{1}{2} \left[\rho A_h \left(R_1^2 l + R_1 l^2 + \frac{l^3}{3} \right) + I_o \right] \quad (7)$$

That system of equations in the state space form of 1^o order can be written as

$$\dot{x}_1 = x_2 \quad (8)$$

$$\dot{x}_2 = \frac{2C_1 C_2 \omega_1^2 x_3 - 2C_1 C_2 x_2^2 x_3 - 8C_1^2 x_2 x_3 x_4 + 2C_1 \xi}{4C_1^2 x_3^2 + C_4} \quad (9)$$

$$\dot{x}_3 = x_4 \quad (10)$$

$$\dot{x}_4 = \frac{4C_1 C_3 x_2^2 x_3 + 4C_1^2 x_2^2 x_3 - 4C_1 C_3 \omega_1^2 x_3 - 4C_1^2 x_3^3 + 4C_1 C_2 x_2 x_3 x_4 - C_2 \xi}{4C_1^2 x_3^2 + C_4} \quad (11)$$

where $C_4 = 4C_1 C_3 - C_2^2$, $x_1 = \theta$, $x_2 = d\theta/dt$, $x_3 = p$ and $x_4 = dp/dt$. The full mathematic development of these equations can be found in the work of Mainenti-Lopes (2008).

The DC motor that will give the control torque is represented in Fig. 3.

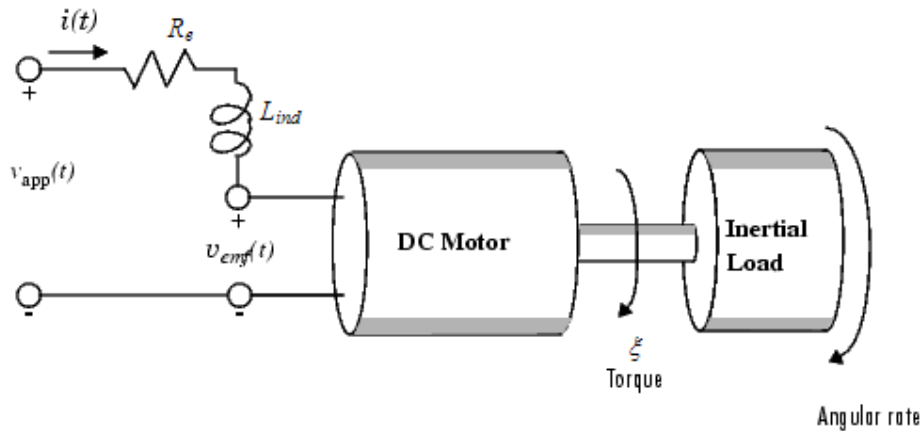


Figure 3. Graphic representation of the DC motor.

In the motor mathematical model, the magnetic field is considered constant. The resistance of the circuit is denoted by R_e and the self-inductance of the armature by L_{ind} . The motor torque is given by

$$\xi = K_m i(t) \quad (12)$$

where K_m is armature constant. The induced electromotive force is a voltage proportional to the angular rate ω that can be described by the following equation

$$v_{emf}(t) = K_b \omega(t) \quad (13)$$

where K_b is the electromotive force constant.

The mechanical part of the motor equations is derived using Newton's laws. The reaction wheel moment of inertia times the derivative of the reaction wheel angular rate equals the motor torque that results the following equation

$$I_R \frac{d\omega}{dt} = \xi = -K_f \omega(t) + K_m i(t) \quad (14)$$

where $K_f \omega$ is a linear approximation of viscous friction. Knowing that the friction is not considered, the Eq. (14) becomes

$$I_R \frac{d\omega}{dt} = K_m i(t) \quad (15)$$

The electrical part of the equations can be described as

$$v_{ap}(t) - v_{emf}(t) = L_{ind} \frac{di}{dt} + R_e i(t) \quad (16)$$

Using this equation in Eq. (12), one can obtained the following system of equations

$$\frac{di}{dt} = -\frac{R_e}{L_{ind}} i(t) - \frac{K_b}{L_{ind}} \omega(t) + \frac{1}{L_{ind}} v_{ap}(t) \quad (17)$$

$$\frac{d\omega}{dt} = \frac{K_m}{I_R} i(t) \quad (18)$$

Including the DC motor equations to the satellite equations, one can be obtained the following equations to the system

$$\dot{x}_1 = x_2 \quad (19)$$

$$\dot{x}_2 = \frac{2C_1 C_2 \omega_1^2 x_3 - 2C_1 C_2 x_2^2 x_3 - 8C_1^2 x_2 x_3 x_4 + 2C_1 K_m x_5}{4C_1^2 x_3^2 + C_4} \quad (20)$$

$$\dot{x}_3 = x_4 \quad (21)$$

$$\dot{x}_4 = \frac{4C_1C_3x_2^2x_3 + 4C_1^2x_2^2x_3 - 4C_1C_3\omega_1^2x_3 - 4C_1^2x_3^3 + 4C_1C_2x_2x_3x_4 - C_2K_mx_5}{4C_1^2x_3^2 + C_4} \quad (22)$$

$$\dot{x}_5 = -\frac{R_e}{L_{ind}}x_5 - \frac{K_b}{L_{ind}}x_6 + \frac{1}{L_{ind}}v_{ap}(t) \quad (23)$$

$$\dot{x}_6 = \frac{K_m}{I_R}x_5 \quad (24)$$

The parameters value of the satellite and a brief description of each parameter are presented in Table 1.

Table 1. Parameters value of the system.

Parameter	Description	Value	Unit
A_h	Cross section of the beam	7.5×10^{-4}	m^2
ρ	Aluminium density	2700	kg/m^3
l	Beam length	1.2	m
E	Young's modulus	7×10^{10}	N/m^2
a_1l	Eigen value associated to the beam first mode of vibration	1.878	-
I_h	Moment of inertia of the beam cross section about the neutral axis	1.5625×10^{-9}	m^4
I_o	Satellite's main body moment of inertia about its center of mass	30.4	$kg.m^2$
ω	Beam first mode of vibration	18,0001	rad/s
R_l	Half of the central body edge	0,5	m
I_R	Reaction wheel moment of inertia	0.0115	$kg.m^2/s^2$
R_e	Resistance of the circuit	2	Ohms
L_{ind}	Self-inductance of the armature	0,5	Henrys
K_m	Armature constant	0.0015	-
K_b	Electromotive force constant	0.0015	-

4 Control Laws

In this work, two control laws were tested: a simple proportional derivative (PD); and a non-linear control law. The PD control law is given by

$$v_{PD} = -K_1x_1 - K_2x_2 \quad (25)$$

and the non-linear control law (Rietz and Inman, 2000) is given by

$$v_{nl} = -K_1x_1 - K_2x_2 - K_3x_1x_2 \quad (26)$$

where K_1 , K_2 and K_3 are gains of the control law. The non-linear term of control law can be interpreted as a time variant damping. Its main function is to reduce the beam vibration using a controller that actuate only in the central body dynamics (Ribeiro, 2005).

Once, the satellite equations are in a proper form for numerical manipulations and the control laws are determinate, the next step is to define the objective functions.

5 Objective functions

The M-GEO_{real} was used to identify the set of gains (K_1 and K_2 for PD and K_1 , K_2 and K_3 for the non-linear control law) that minimize the time to control the satellite and the energy spent by the controller, considering that the initial attitude angle is 28.65° and the desired final attitude angle is 0° .

In order to integrate the equations of motion, one uses the fourth order Runge-Kutta algorithm (RK4). For each set of gains tried by M-GEO_{real}, it called the RK4 algorithm that allowed to calculate the value of energy spent and time to control de satellite using the following equations

$$F_1 = T \quad (27)$$

$$F_2 = \sum_{l=0}^{hT} |\xi \cdot \Delta \theta_l| \quad (28)$$

One can use the Eq. (12) in Eq. (28) and write as

$$F_2 = \sum_{l=0}^{hT} |K_m \cdot i(t) \cdot \Delta \theta_l| = \sum_{l=0}^{hT} \left| \frac{K_m}{R_e} \cdot v(t) \cdot \Delta \theta_l \right| = \sum_{l=0}^{hT} \left| \frac{K_m}{R_e} \cdot v(t) (x_{1l} - x_{1l+1}) \right| \quad (29)$$

where T is the instant that the satellite is controlled. In other words, the instant that fulfill the following conditions: $|\theta| < 0.1^\circ$ and $|\dot{\theta}| < 0.03^\circ/\text{s}$. h is the step of RK4, x_{1l} is the angle shift and of each i-th iteration of RK4 and $v(t)$ is the input voltage ($v_{PD}(t)$ for PD and $v_{nl}(t)$ for non-linear control law). That is, the energy spent by the controller. The side constraints were $0 < K_1 < 20000$, $0 < K_2 < 20000$ and $0 < K_3 < 20000$.

6 Simulation results

The M-GEO_{real} performance was compared to the LQR method (Stengel, 1994). The LQR method can be treated as weighed sum method. Therefore, if one wants to recover all Pareto Front, it is necessary to run the LQR method several times with different set of weigh. Besides, weighed sum methods cannot recover non-convex Pareto Front (Messac *et al.*, 2000). In this work, only one solution of LQR will be used.

In other to apply the LQR method, one needs to make linearization in the satellite equations, considering the deflections and the velocities small. Such linearization is not necessary to apply M-GEO_{real}, since this algorithm is able to approach non-linear problems.

The τ values were tested from 1 to 10, with variation 0.5 between each τ tested and all others parameters fixed in $\sigma_I = 1$; $P = 2$ e $rt = 20$. Once, the best value for τ was determined, this parameter was fixed and the others were tested according with the following order: P ; σ_I and rt . The values tested for these parameters were: $P = 2, 3$ and 4 ; $\sigma_I = 1$ and 2 ; and $rt = 10, 20, 30, 40$

and 50. The N value is associated with the used control law ($N = 2$, for PD and $N = 3$ for non-linear control law).

The weighting matrices for LQR method considered here were

$$Q = \begin{pmatrix} 10^4 & 0 & 0 & 0 & 0 & 0 \\ 0 & 10^4 & 0 & 0 & 0 & 0 \\ 0 & 0 & 100 & 0 & 0 & 0 \\ 0 & 0 & 0 & 100 & 0 & 0 \\ 0 & 0 & 0 & 0 & 0 & 0 \\ 0 & 0 & 0 & 0 & 0 & 0 \end{pmatrix} \quad (30)$$

and

$$R = (1) \quad (31)$$

One can obtain the following gains using the LQR() routine of MATLAB: $K_{x1} = 100$; $K_{x2} = 3021.3$; $K_{x3} = 243.1$ and $K_{x4} = 232.2$.

Figure 4 shows the comparison of performance between M-GEO_{real} algorithm and LQR method. The Pareto Front obtained with PD control law is presented with red square, the non-linear control law with blue lozenge and the green triangle is the LQR solution.

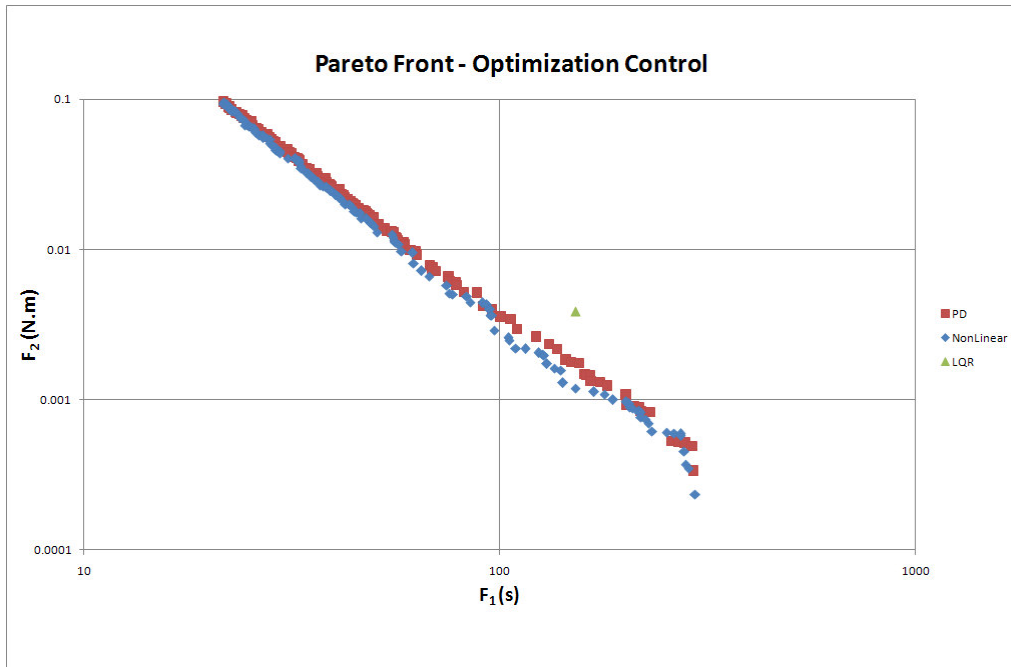


Figure 4. Pareto Front for the problem presented in section 3 with a PD control law in red square, with non-linear control law in blue lozenge and the LQR solution.

The M-GEO_{real} was able to return Pareto Fronts that several of its solutions dominate the solution generate by LQR. The capacity of M-GEO_{real} to approach non-linear problems is a possible explanation of the better performance of this algorithm. On the other hand, the LQR method can be applied only to linear problems, so its solution is sub-optimal for the non-linear problems.

Comparing the Pareto Front of the two control laws used in this work, one can observe that for low energy the non-linear control law consumes less energy than the PD control law. Therefore, the Pareto Front of non-linear control law dominates the other Pareto Front in that region. While, in the region of high energy, the use of energy is the same between the two control laws. That is, for situation that is necessary to control the satellite in sort time, there is no advantage to use the non-linear control law.

7 Conclusions

In this work, M-GEO_{real} algorithm was applied to an optimization of attitude control law of a rigid-flexible satellite and its efficiency was compared to the LQR method. The satellite was modeled as central rigid body with a clamped-free beam free to rotate in only one axis. This system was controlled by a reaction wheel driven by a DC motor. Two control laws were tested: a PD and; a non-linear control law. The function of M-GEO_{real} was to determine gains to these control laws that minimize, simultaneously, the time to control the satellite and the energy to do this job.

As result, the M-GEO_{real} successfully recovered the Pareto Front for the two control laws. Several solutions obtained by M-GEO_{real} dominated the solution generate by LQR. Considering that LQR is a linear method, one needed to linearize the satellite equations to apply this method. Therefore, the gains obtained by LQR was sub-optimize for the non-linear system.

A comparison between PD and non-linear control law showed that for high consumption of energy the PD control law was as efficient as the non-linear control law. On the other hand, for low use of energy the non-linear control law had showed better performance. Concluding, M-GEO_{real} was successfully applied to optimal attitude control problem, showing that it is an alternative algorithm to tackle such kind of problem.

8 References

- Davis, L. D., De Jong, K., Vose, M. D., and Whitley, L. D., 1999, "Evolutionary Algorithms", Mathematics and Its Applications, Vol. 111, Springer-Verlag, Berlin, Germany.
- De Sousa, F. L., Ramos, F. M., Paglione, P. and Girardi, R. M., 2003, "New Stochastic Algorithm for Design Optimization", AIAA Journal, Vol. 41, No. 9, pp. 1808 –1818.
- De Sousa, F. L., Vlassov, V. and Ramos, F. M., 2004, "Heat Pipe Design Through Generalized Extremal Optimization", Heat Transfer Engineering, Vol. 25, Number 7 (Selected 271 papers from the 9th Brazilian Congress of Thermal Sciences and Engineering), pp. 34 -45, (ISSN 0145-7632).
- De Souza, L. C. G., 2006, "Satellite Attitude Control Systems Parameters Optimization", Proceedings of the 3rd European Conference on Computational Mechanics Solids, Structures and Coupled Problems in Engineering, Lisbon, Portugal, pp. 5 –8.

- Ge, X. S. and Chen L. Q., 2004, "Attitude Control of a Rigid Spacecraft with Two Momentum Wheel Actuators Using Genetic Algorithm", *Acta Astronautica*, 55, pp. 3 –8.
- Hughes, P. C., 1986, "Spacecraft Attitude Dynamics", John Wiley & Sons, Inc.
- Mainenti-Lopes I., De Sousa, F. L., Souza, L. C. G., 2008, "The Generalized Extremal Optimization with Real Codification", *Proceedings of the EngOpt 2008 - International Conference on Engineering Optimization*, Rio de Janeiro, Brazil.
- Mainenti-Lopes I., De Sousa, F. L., Souza, L. C. G., Cuco, A. P. C., 2009, "Multi-Objective Generalized Extremal Optimization With Real Codification And Its Application In Satellite Attitude Control", *Proceedings of the 20th International Congress of Mechanical Engineering*, Gramado, RS, Brazil.
- Messac, A.; Sundararaj, G.J.; Tappeta, R.V.; Renaud, J.E. Ability of objective functions to generate points on nonconvex Pareto frontiers. *Optimization*, v. 38, n. 6, p. 1084-1091, 2000.
- Rezende, C. P., Fenili, A.; Souza, L. C. G., 2004, "Modelagem e Controle de Estruturas Flexíveis - Abordagem Ideal e Não Ideal: Caso Linear", *Proceedings of the 3rd Brazilian Conference on Dynamics, Control and Applications - DINCON*, Ilha Solteira.
- Rietz R. W., Inman, D. J., 2000, "Comparison of Linear and Nonlinear Control of a Slewing Beam". *Journal of vibration and control*, Vol. 6, No. 2, pp. 309 - 322.
- Ribeiro, J. E. S., 2005, "Controle não linear de uma estrutura flexível (curvatura linear) considerando fonte de potência ideal e não ideal", *Proceedings of the Seminário de Iniciação Científica do INPE (SICINPE)*, São José dos Campos.
- Stengel, R. F., 1994, *Optimal Control and Estimations*, Dover publications, inc.